EEET ECOLOGICAL ENGINEERING & ENVIRONMENTAL TECHNOLOGY

Ecological Engineering & Environmental Technology 2024, 25(11), 353–364
https://doi.org/10.12912/27197050/193076
ISSN 2299–8993, License CC-BY 4.0

Received: 2024.08.20
Accepted: 2024.09.15
Published: 2024.10.01

Study and Analysis of Flow Regime Transitions in Straight Channels Using the Lattice Boltzmann Method for Shallow Water

Ibrahim El Ghazali[1], Anass Bendaraa[1*], Moulay Mustapha Charafi[1]

[1] LS2ME Laboratory, Polydisciplinary Faculty of Khouribga, Sultan Moulay Slimane University of Beni Mellal, B.P. 145, Khouribga 25000, Morocco

* Corresponding author's e-mail: anass.bendaraa@gmail.com

ABSTRACT

The objective of this work is to examine the unexplored dynamics of flow regime changes in linear channels, with a specific emphasis on the impact of relaxation time, channel width, and external forces on the shift from laminar to turbulent flow. This study intends to improve understanding of how the parameters associated with the Lattice Boltzmann model for shallow water equations (LABSWE) can be modified to change flow regimes using a D2Q9 approach for domain discretization. Our investigations demonstrate that a decrease in relaxation time prompts a shift from a parabolic (laminar) to a logarithmic (turbulent) velocity distribution, evidenced by significant fluctuations in the central channel velocity and an increase in the Reynolds number. This study also reveals that broader channel widths lead to turbulent flow, marking a notable departure from the laminar flow observed in narrower settings. The application of external forces further intensifies this transition, showcasing their pivotal role in influencing flow regimes. This study presents significant scientific novelty by offering new insights into the conditions that foster flow regime transitions, thereby addressing a gap in the current fluid mechanics literature. Our findings suggest practical ways to manipulate these factors to optimize flow behaviors, providing valuable insights for the engineering and environmental management of water systems.

Keywords: shallow water equations; Lattice Boltzmann method; LABSWE; laminar and turbulent flow; flow in straight channels.

INTRODUCTION

Studying fluid flow in channels is an essential aspect of fluid dynamics. These channels represent various natural and artificial systems and serve as crucial components in several domains such as water supply, wastewater treatment, industrial operations, and flood control activities. Notably, research on the flow of shallow waters in these channels is crucial for optimizing various practical applications. Understanding the dynamics of shallow flows allows for improved design and management in systems such as water supplies, industrial processes, and flood control, highlighting the importance of research in this domain. In addition, much research has focused on transitions between flow regimes in channels, with practical and numerical studies concentrating on critical aspects of fluid dynamics within channels affected by the nature of the flow with significant practical implications (Hashemi et al., 2018; Liu et al., 2018; Pargal et al., 2021). An investigation of these regime shifts, such as the shift from laminar to turbulent flow, is essential for designing and operating hydraulic systems and predicting changes affecting transport and fluid flow processes. Historically, efforts to simulate and study these flows have heavily depended on solving the Navier-Stokes equations. While these equations provide robust insights into fluid behavior, their computational intensity, especially for complex flow scenarios, often poses challenges. This led to the search for alternative numerical methods to simulate fluid flow while maintaining accuracy efficiently. Among the emerging techniques, in recent years, the lattice Boltzmann method (LBM) has gained significant prominence.

A computational method for simulating fluid dynamics is the lattice Boltzmann method (LBM) (Chen et al., 1998). The formulation is derived from the Boltzmann equation, which characterizes the flow of a fluid at a microscopic scale by considering the dispersion of particle velocities. Originally derived from the lattice gas automata (Benzi et al., 1992), the LB technique was enhanced in terms of efficiency and simplicity by the incorporation of the Bhatnagar-Gross-Krook (BGK) scheme (Qian et al., 1992).

In LBM, the fluid is represented as a lattice of nodes, with each node holding information about the local fluid properties such as velocity and density. The method uses a set of simple collision and streaming rules to update the state of each node at discrete time steps. Although For solving shallow water equations, researchers prefer the fractional boundary method (LBM) over the finite difference (Fennema et al., 1990), finite volume (Yoon et al., 2004), and finite element methods (Liang et al., 2008), because of its simplicity, efficiency, and capacity to handle boundary conditions (Chen et al., 2021; Isabelle Cheylan, Julien Favier, 2021; Ningning Wang, Wanglai Ni, 2024).

The use of the lattice Boltzmann approach to several flow issues has shown its capacity, precision, and potential in accurate simulation of shallow water flows (Peng et al., 2011; Venturi et al., 2020; De Rosis, 2023). One of the seminal investigations in this domain is the research undertaken by Zhou (Zhou, 2002). He devised Lattice Boltzmann models, (LABSWE and LABSWE™), for shallow water equations, both with and without turbulence modeling. He exemplified the simplicity, efficacy, and precision of their solutions to shallow water equations.

Although the mathematical modeling, simulation methods, and domain discretization techniques employed in this study are based on well-established methodologies like the Lattice Boltzmann Model (LABSWE) and the D2Q9 lattice scheme, the innovation of this work lies in their novel application to the specific and underexplored problem of flow regime transitions in straight channels under shallow water conditions. This research focuses on understanding how small changes in key parameters, such as relaxation time, channel width, and external forces, can significantly impact the stability and behavior of flow, a topic that has not been thoroughly examined in this context.

The aim of this work is to carefully examine the impact of relaxation time, channel width, and external forces on the transition from laminar to turbulent flow. By manipulating these parameters, we want to establish control over this transition. This control is crucial for optimizing hydraulic systems, as it allows engineers to design channels that minimize turbulence-induced erosion and ensure stable, efficient flow. Furthermore, controlling these parameters is vital in applications such as flood management, where maintaining a stable flow regime can prevent the sudden onset of turbulence that could lead to infrastructure failure.

PHYSICAL MODEL DESCRIPTION

The current lattice Boltzmann model, specifically designed for shallow water flows, has been implemented on a linear channel, as depicted in Figure 1. In order to define the initial conditions of our investigation, we specify the discharge (Q) at the entrance of the channel and the water depth (h) at the downstream end. In order to accurately represent the interaction between the fluid and the lateral walls of the channel, we implement no-slip boundary conditions.

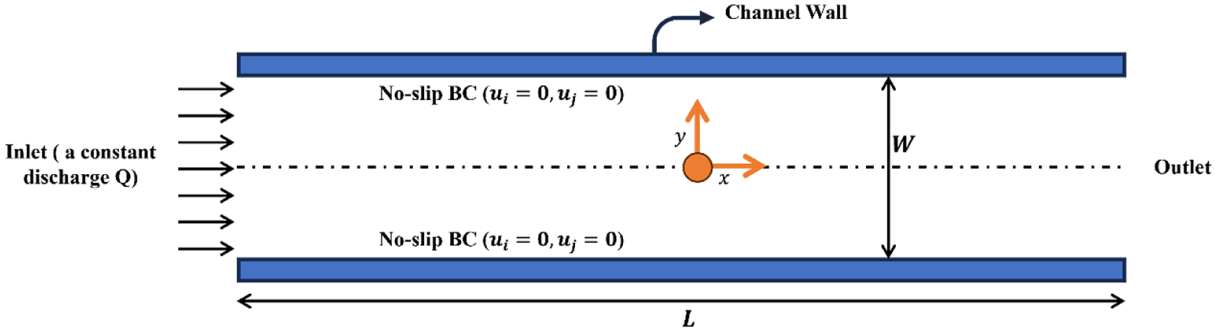

Figure. 1. Diagram showing flow in a straight channel

Lattice Boltzmann shallow water equation model (LABSWE)

This section describes the Lattice Boltzmann Model for Shallow Water Equations (LABSWE). First, the 2D Shallow Water Equations (SWE) overview is presented. Then, the Lattice Boltzmann Equation (LBE) is formulated to solve the SWE numerically. After that, boundary conditions for a straight channel case are implemented. Finally, the solution process for the LABSWE method is elucidated through a computational flowchart.

Shallow water equations

The shallow water equations are an ensemble of hyperbolic partial differential equations that characterize fluid dynamics in shallow aquatic environments. Their derivation from the Navier-Stokes equations enables their application in the modeling of diverse geophysical flows, including tides, storm surges, river flows, and tsunamis. A defining feature of shallow water flows is their significantly larger horizontal length scale compared to the vertical length scale. The shallow water equations in two dimensions expressed as:

$$\frac{\partial h}{\partial t} + \frac{\partial (hu_i)}{\partial x_i} = 0 \tag{1}$$

$$\frac{\partial (hu_i)}{\partial t} + \frac{\partial \left(hu_i u_j\right)}{\partial x_j} = \\ = -g\frac{\partial}{\partial x_i}\left(\frac{h^2}{2}\right) + v\frac{\partial^2 (hu_i)}{\partial x_j \partial x_j} + F_i \tag{2}$$

where: h the water depth, t the time, i and j space direction indices, u_i the velocity, F_i the force term, defined as

$$F_i = -gh\frac{\partial z_b}{\partial x_i} - \frac{\tau_{bi}}{\rho} \tag{3}$$

where: z_b the bed elevation, g the gravitational acceleration, and τ_{bi} the bed shear stress are determined by

$$\tau_{bi} = \rho C_b u_i \sqrt{u_j u_j} \tag{4}$$

where: C_b is the bed friction coefficient defined as

$$C_b = \frac{g n_b^2}{h^{\frac{1}{3}}} \tag{5}$$

where: n_b is Manning's coefficient.

The conventional version of the lattice Boltzmann equation on the 9-speed square lattice depicted in Figure 2 is:

$$f_\alpha(x + e_\alpha \Delta t, t + \Delta t) - f_\alpha(x,t) = \\ = -\frac{1}{\tau}\left[f_\alpha(x,t) - f_\alpha^{eq}(x,t)\right] + \frac{\Delta t}{6e^2} e_{\alpha i} F_i(x,t) \tag{6}$$

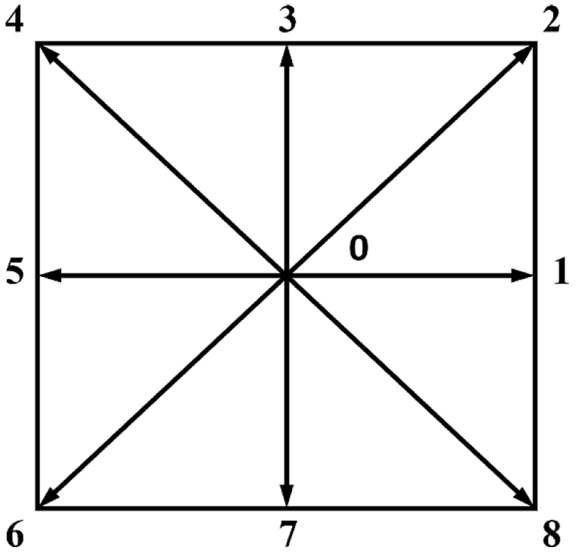

Figure 2. 9-Speed square lattice

where: f_α is the distribution function of particles; F_i is the component of the force in i direction; τ is the relaxation time; $e = \frac{\Delta x}{\Delta t}$; Δx is the lattice size, and Δt is the time step, e_α is the particle velocity in link α, which is defined by:

$$e_\alpha = \begin{cases} (0,0), & \alpha = 0 \\ e\left[cos\frac{(\alpha-1)\pi}{4}, sin\frac{(\alpha-1)\pi}{4}\right], & \alpha = 1,3,5,7 \\ \sqrt{2}e\left[cos\frac{(\alpha-1)\pi}{4}, sin\frac{(\alpha-1)\pi}{4}\right], & \alpha = 2,4,6,8 \end{cases} \tag{7}$$

f_α^{eq} is the local equilibrium distribution function is officially defined as:

$$f_\alpha^{eq} = \begin{cases} h - \frac{5gh^2}{6e^2} - \frac{2h}{3e^2}u_i u_i, & \alpha = 0 \\ \frac{gh^2}{6e^2} + \frac{h}{3e^2}e_{\alpha i}u_i + \frac{h}{2e^4}e_{\alpha i}e_{\alpha j}u_i u_j - \frac{h}{6e^2}u_i u_i, & \alpha = 1,3,5,7 \\ \frac{gh^2}{24e^2} + \frac{h}{12e^2}e_{\alpha i}u_i + \frac{h}{8e^4}e_{\alpha i}e_{\alpha j}u_i u_j - \frac{h}{24e^2}u_i u_i, & \alpha = 2,4,6,8 \end{cases} \tag{8}$$

A combination of the lattice Boltzmann Equation 3 and the local equilibrium function (5) is employed to solve Equations 1 and 2 relevant to shallow water. These components together provide a lattice Boltzmann model for shallow water flows (LABSWE) on square lattices, as defined by Zhou (Zhou, 2002).

The solutions to Equations 1 and 2, yielding the physical constants water depth h and velocity u_i, can be computed using Equations 9 and 10, respectively (Zhou, 2004).

$$h = \sum_\alpha f_\alpha \tag{9}$$

$$u_i = \frac{1}{h}\sum_\alpha e_{\alpha i} f_\alpha \tag{10}$$

Boundary conditions

The solution of the shallow water equations necessitates the application of specific boundary conditions. The transformation of these conditions into appropriate boundary conditions for the LABSWE is important. The following subsections outline the suitable boundary conditions for the problem being investigated:

Inflow, outflow boundary conditions

In the LBM framework, the distribution functions at the boundary nodes require careful treatment, as they cannot be directly obtained from the lattice nodes within the computational domain. At the inflow boundary, the distribution functions f_1, f_2, and f_8 along the line $\overline{AD}$ (as shown in Fig. 3 are unknown after the streaming step. To determine these values, we apply a zero-gradient condition normal to the boundary, a method commonly used in LBM simulations. This zero-gradient condition implies that the distribution function at the boundary node is set equal to the value at the adjacent internal node. Specifically, the distribution functions at the inflow boundary are updated as follows:

$$f_\alpha(1,j) = f_\alpha(2,j), \alpha = 1,2,8 \quad (11)$$

Similarly, for the outflow boundary $\overline{BC}$ as depicted in Figure 3, the relationships for f_4, f_5, and f_6 can be given by:

$$f_\alpha(N_x,j) = f_\alpha(N_x-1,j), \alpha = 4,5,6 \quad (12)$$

The entire lattice number in the x direction is denoted as N_x.

Zou and He (Zou et al., 1997) proposed a theory to determine the unknown distribution function f_α at the border when the velocity and depth are known. For instance, by considering the velocity at the inflow boundary, it is possible to determine the unknown values of f_1, f_2, and f_8 after streaming:

$$f_1 = f_5 + \frac{2hu}{3e} \quad (13)$$

$$f_2 = \frac{hu}{6e} + f_6 + \frac{f_7 - f_3}{2} \quad (14)$$

$$f_8 = \frac{hu}{6e} + f_4 + \frac{f_3 - f_7}{2} \quad (15)$$

Solid boundary conditions

Accurate simulation of the interaction between fluid and solid surfaces in LBM strongly relies on the inclusion of solid boundary conditions. Commonly applied conditions include two types: no-slip and slip boundary conditions.

Under situations of no-slip, the bounce-back scheme is commonly used. Within this particular design, the distribution functions that go towards a solid boundary undergo reflection in the opposite direction during the streaming step. As mandated by the no-slip boundary condition, this reflection takes place at the lattice node next to the boundary, therefore imposing a zero-velocity requirement at the wall.

Slip boundary conditions eliminate friction and resistance, therefore enabling fluid motion along the boundary. This phenomenon is represented by imposing a zero-gradient condition on the distribution function that is normal to the solid boundary. This implies that the value of the distribution function remains constant when approached perpendicular to the boundary. This state replicates a situation in which the fluid assumes no shear stress at the boundary, therefore enabling it to move through a slide down the surface. In practice, these boundary conditions are implemented as follows:

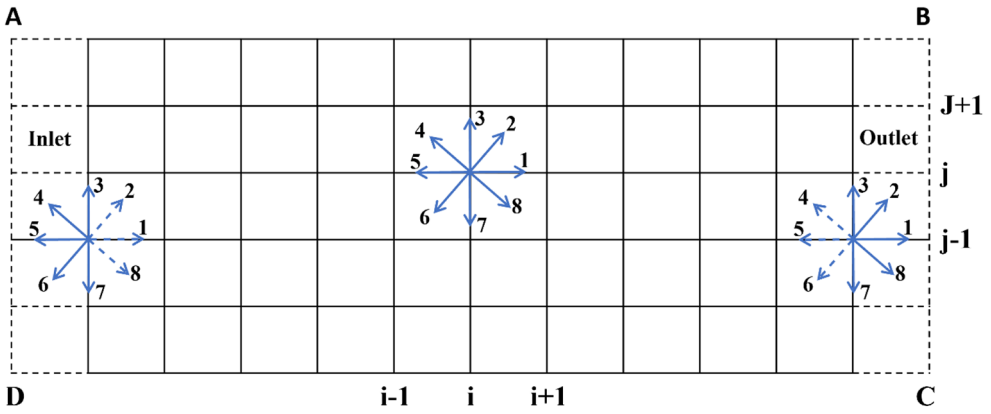

Figure 3. Lattice node inflow/outflow boundary definition sketch

- the no-slip condition (Bounce-Back) states that when a distribution function f_α is oriented towards a solid boundary, it will be reflected back as $f_{\bar{\alpha}}$, where $\bar{\alpha}$ represents the opposite direction. Consequently, the no-slip condition is satisfied as the macroscopic velocity at the border remains zero.
- slip condition (zero gradient) - in slip boundaries, the distribution functions are modified to ensure that the gradient perpendicular to the boundary is zero, indicating that the distribution function at the boundary is equivalent to the distribution function at adjacent internal node.

These methods ensure that the solid boundaries are accurately represented, preventing unphysical behaviors such as fluid penetration or artificial boundary effects that could compromise the simulation's accuracy.

Solution procedure

For LABSWE, the resolution method is straightforward and is outlined in Figure 4.

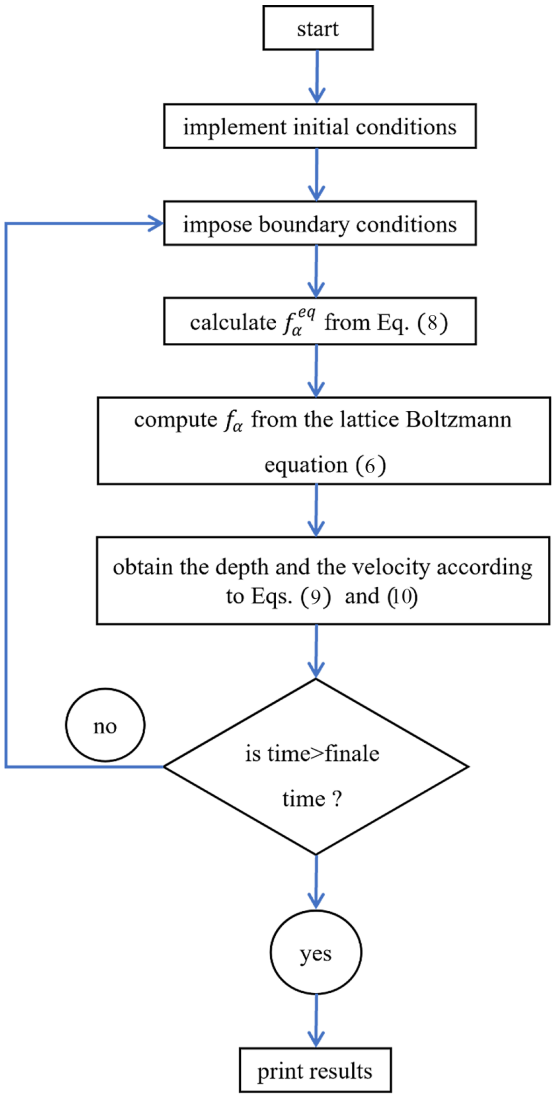

Figure 4. LABSWE model flowchart

RESULTS AND DISCUSSIONS

Effect of relaxation time

In this section, we investigate the influence of relaxation time, a critical parameter in fluid dynamics, which is intrinsically linked to the fluid's viscosity via the relationship:

$$v = \frac{1}{3}\left(\tau - \frac{1}{2}\right) \tag{16}$$

This indicates that studying relaxation time is like studying viscosity. The lattice Boltzmann model for shallow water equations (LABSWE) with a D2Q9 lattice was used to simulate a straight channel 6m long and 0.6m wide. The relaxation times were set to τ = 0.55, τ = 0.54, τ = 0.53, τ = 0.52, τ = 0.51, τ = 0.507 and τ = 0.501. The channel simulations used an inflow discharge of Q = 0.0123 $m^3 \cdot s^{-1}$, and a downstream water depth of h = 0.05 m. Δx and Δt are considered to be 0.02 m and 0.004 s, respectively. No-slip boundary criteria are applied on wall sides.

The velocity distribution at the cross section for different relaxation time values is depicted in Figure 5. At higher relaxation times, the distribution is parabolic, characteristic of laminar flow. However, as the relaxation time decreases, the distribution becomes logarithmic, indicating a transition to turbulent flow. This transition is intrinsically linked to the relationship between relaxation time and viscosity in the fluid (Eq. 16). A reduction in the relaxation time results in a corresponding drop in the viscosity of the fluid, thereby causing an elevation in the Reynolds number, as presented in Figure 6. This phenomenon arises due to the fact that the Reynolds number is a dimensionless parameter that exhibits an inverse relationship with viscosity. In particular, the Reynolds number is determined by the Equation

$$Re = \frac{UL}{v} \tag{17}$$

where: U represents the characteristic velocity, L represents the characteristic length, and v represents the kinematic viscosity.

As viscosity decreases, the Reynolds number increases, driving the transition from a laminar regime, characterized by a parabolic velocity profile,

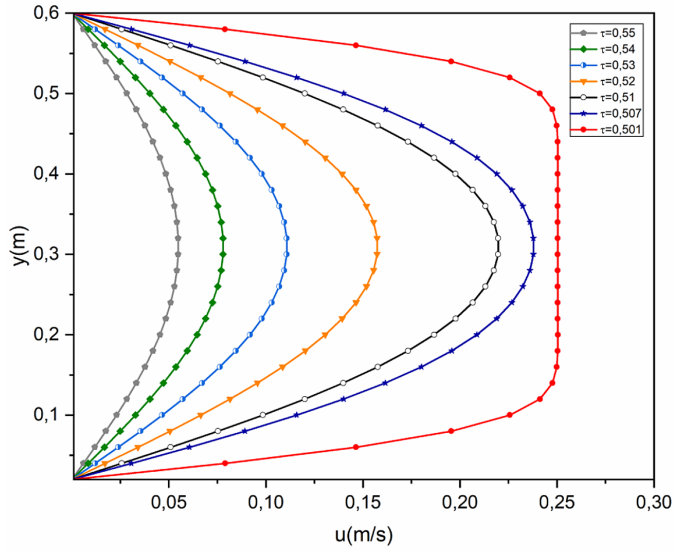

Figure 5. Velocity distribution at the cross-section for different relaxation times.

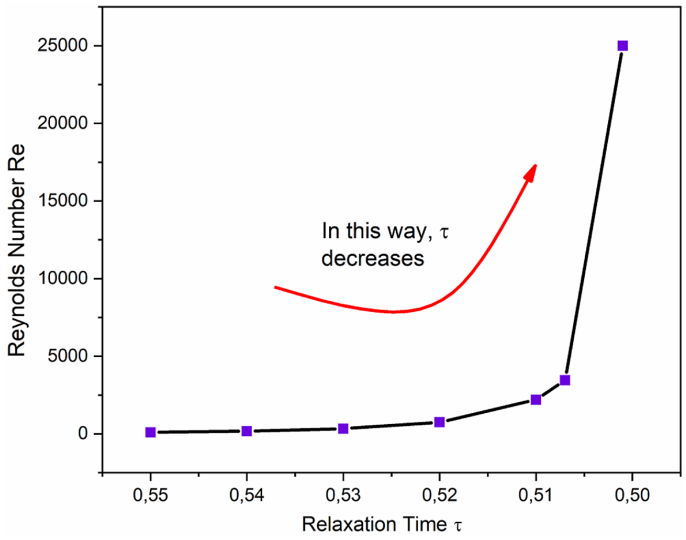

Figure 6. Variation of reynolds number with relaxation time τ

to a turbulent regime. In flows with high Reynolds numbers, inertial forces become more significant than viscous forces, leading to a logarithmic velocity distribution profile. This logarithmic profile is a defining feature of turbulent flows. Through the analysis of the temporal development of the velocity at the center of the channel for two distinct relaxation times, $\tau = 0.55$ and , $\tau = 0.501$, as shown in Figures. 7 and 8, the apparent shift from laminar to turbulent flow regimes is verified. For a value of 0.55, the velocity near the central point of the channel remained constant at 0.25 $m \cdot s^{-1}$ before progressively decelerating. Internal viscous forces, which disperse the fluid's kinetic energy when no external forces propel the flow, cause the diminution in velocity. When the relaxation period was reduced to $\tau = 0.501$, significant variations in the velocity near the channel's center were observed, indicating a significant degree of flow instability. The oscillations seen and the logarithmic shape of the velocity distribution at the cross-section are strong proof that the flow regime changed from laminar to turbulent.

Effect of channel width

To examine the impact of the width of a straight channel on flow properties, the LABSWE model with a D2Q9 lattice was employed. The length of the channel was maintained at 6 m,

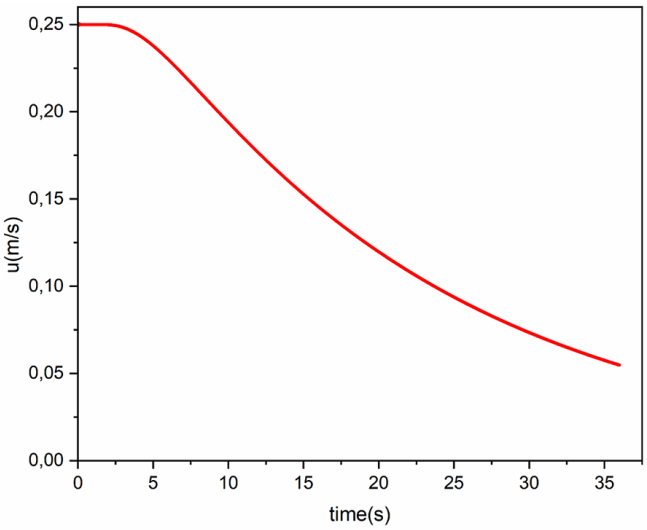

Figure 7. Temporal evolution of the channel center velocity with $\tau = 0.55$

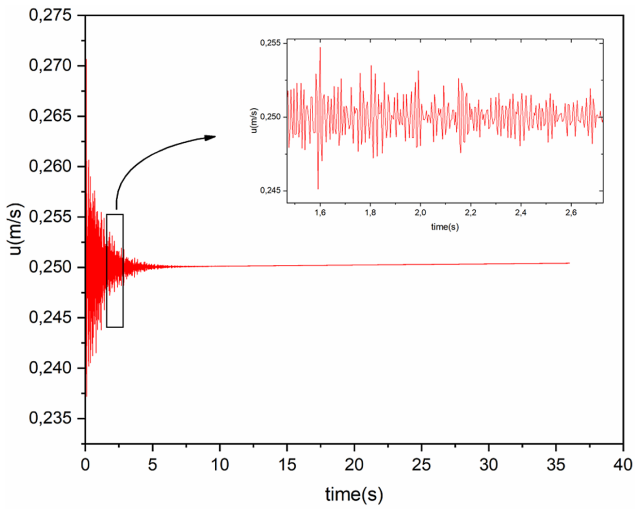

Figure 8. Temporal evolution of the channel center velocity with $\tau = 0.501$

while the width was gradually raised in a sequence of increments: 0.6 m, 1 m, 1.4 m, 1.8 m, 2.2 m, and 5.4 m. The numerical calculations were conducted with a discharge charge of Q = 0.0123 $m^3 \cdot s^{-1}$, at the inflow and a predetermined h value of 0.05 m at the downstream end. Δx = 0.02 m, Δt = 0.004 s, and τ = 0.55. Non-slip boundary conditions were imposed on the side walls.

The influence of the width of the channel on the distribution of velocity in the cross-section is illustrated in Figure 9. The analysis of this image reveals that the channel width has a crucial influence on the flow dynamics in this particular arrangement. Furthermore, the correlation between Reynolds number (Re) and channel width is crucial for studying the shift of flow from laminar to turbulent. Reynolds number is defined as the ratio of the fluid density to the dynamic fluid viscosity.

$$Re = \frac{\rho u D}{\mu} \tag{18}$$

where: ρ is the fluid density, u is the fluid velocity, D is the characteristic length (channel width), and μ is the effective fluid viscosity.

Smaller Reynolds numbers in narrower channels suggest a scenario in which viscous forces outweigh inertial forces. These conditions lead to a laminar flow that is defined by a parabolic distribution of velocity in the channel. The Reynolds number increases proportionally with the channel width, as depicted in Figure 10. Once the value of Re beyond a specific threshold, the flow undergoes a transition from a laminar to a turbulent

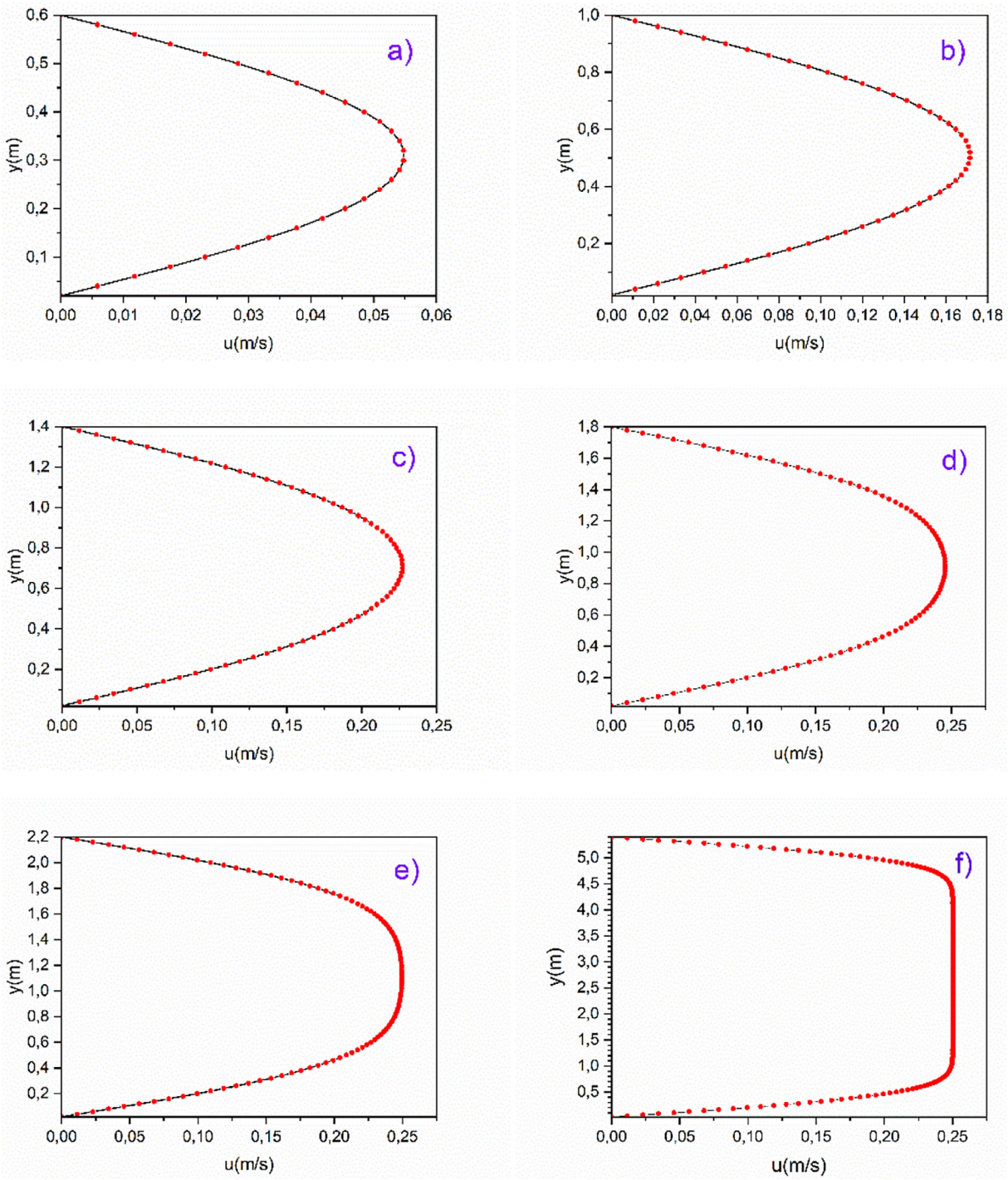

Figure 9. Velocity distribution at the cross-section for different channel widths: (a) 0.6 m, (b) 1 m, (c) 1.4 m, (d) 1.8 m, (e) 2.2 m, (f) 5.4 m

regime. This transition is accompanied by a shift in velocity distribution from a parabolic to a logarithmic profile due to the substantial impact of inertial forces on the material flow.

Effect of external forces

This section examines the impact of external forces on the flow dynamics in a linear channel using the LABSWE method. This study examines the impact of external influences on the velocity and depth of flow in the x and y directions.

The channel has dimensions of 6 m in length and 1.5 m in width. Application of a constant force in the x-direction $f_x = 0.000171\ N$ and in the y-direction $f_y = 0.000012\ N$ is seen. A discharge defines the inlet $Q = 0.0123\ m^3 \cdot s^{-1}$ and a fixed water depth of 0.05 m is established at the

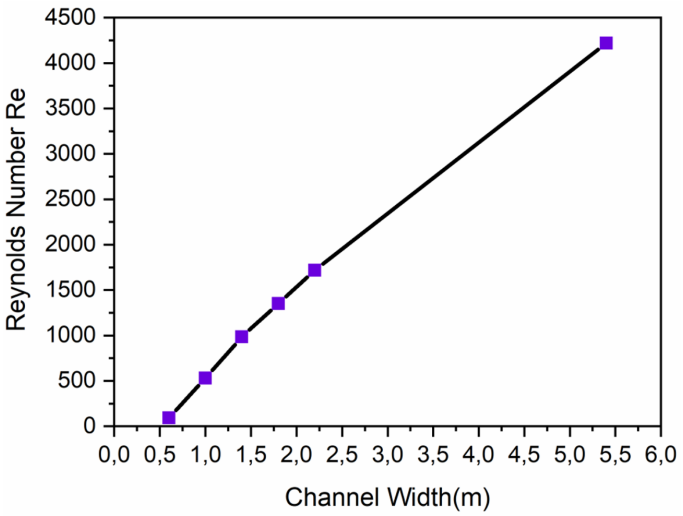

Figure 10. Variation of Reynolds number with channel width.

downstream exit according to the discharge. Application of no-slip boundary conditions is implemented along the side walls. The parameters Δx, Δt, and τ are given values of 0.02 m, 0.004 s, and 0.55, respectively.

In the absence of external forces ($fx = fy = 0$), the flow exhibited a parabolic velocity profile, as shown in Figure 11, characteristic of laminar flows. The Reynolds number, in this case, is Re = 1078. However, with the application of external forces fx = 0.000171 N and fy = 0.000012 N, the velocity profile underwent an apparent transformation, as illustrated in Fig. 12, showing a logarithmic distribution indicating a transition to the turbulent regime. What confirms this transition is the increase in the Reynolds number to Re = 140625.

Applying external forces increases fluid velocity, thereby elevating the Reynolds number. When this number exceeds a certain threshold, inertial forces dominate viscous forces, causing the flow to transition from laminar to turbulent.

In addition, the constant depth of the fluid observed without external forces (Fig. 13) becomes variable when the force is applied (Fig. 14). This difference is linked to the appearance of a pressure gradient due to these forces. When external forces are applied to the fluid, they create zones of non-uniform pressure. The resulting pressure gradient causes the fluid to move, accelerating the flow in certain regions. In the context of fluid dynamics, flow acceleration in certain areas leads to localized decreases in fluid depth due to the principle of conservation of mass. At the same time, decelerations

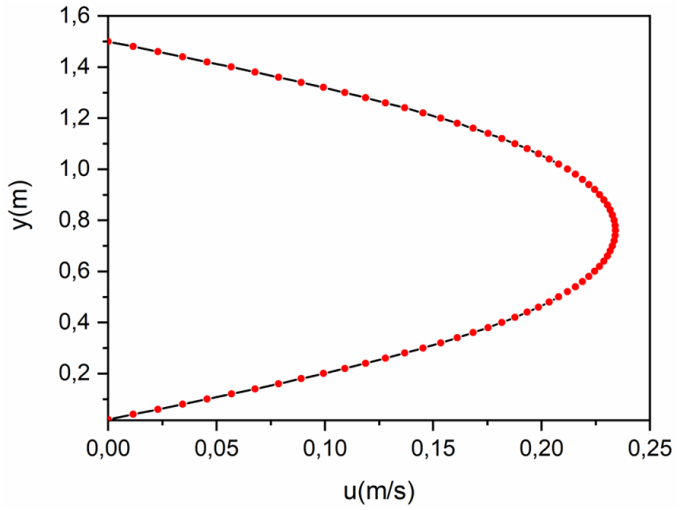

Figure 11. Channel velocity profile without external forces

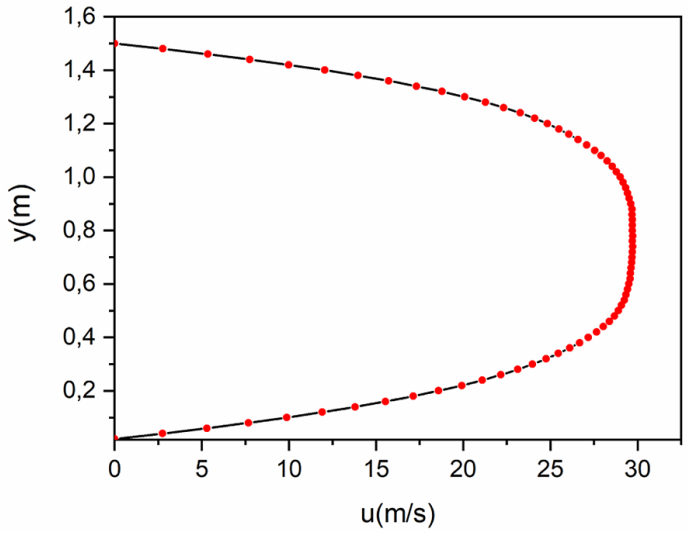

Figure 12. Channel velocity profile under external forces

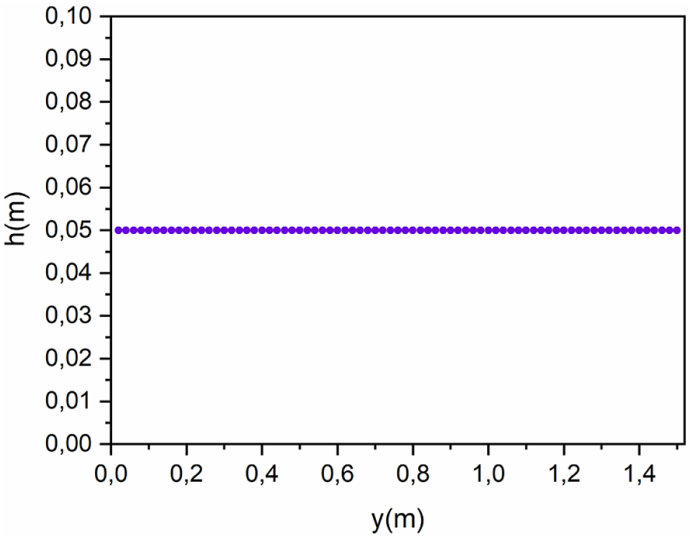

Figure 13. Fluid depth in the channel without external forces

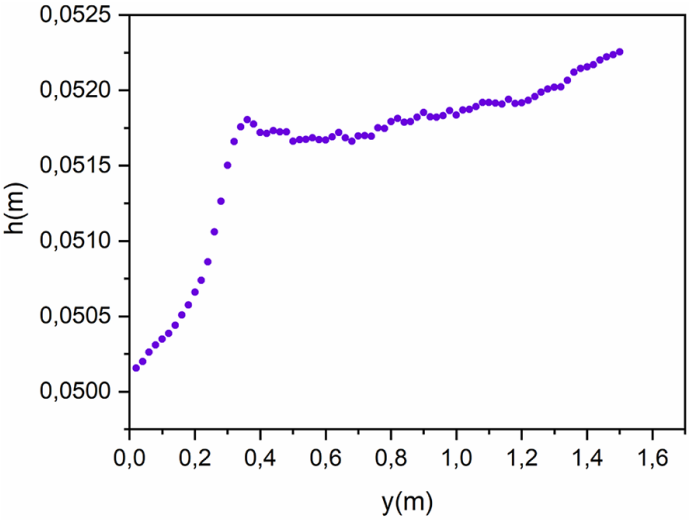

Figure 14. Fluid depth in the channel under the effect of external forces.

or lateral displacements can cause depth increases in other regions. Fluid depth variation is, therefore, a direct reflection of fluid dynamics under pressure triggered by external forces.

CONCLUSIONS

This research successfully delineates the effects of relaxation time, channel width, and external forces on the transition between laminar and turbulent flow regimes in straight channels. We found that reducing relaxation time not only accelerates the transition but also instigates pronounced fluctuations in central channel velocities, a phenomenon less documented in existing studies. Similarly, our findings regarding the role of channel width provide new quantitative insights into how much widening a channel influences the onset of turbulence, providing a clearer understanding of the critical dimensions necessary for such transitions. Additionally, introducing external forces as a variable in our experiments revealed their potent effect in hastening the laminar-turbulent transition, filling a critical knowledge gap regarding the direct manipulation of flow behavior through external stimuli.

This study bridges a significant gap by quantitatively linking changes in flow behavior to specific alterations in physical channel conditions and external force applications, enhancing our understanding of flow dynamics that could guide the design and management of hydraulic systems and environmental flows.

Looking forward, these findings open prospects for further research into the scalability of these effects in larger or more complex channel systems and their applicability in real-world scenarios, such as flood management and environmental conservation.

REFERENCES

1. Bazilevs Y.H., Kiendl M., Wüchner J., Rand Bletzinger K. 2008. Numerical Modeling of Turbulent Compound Channel Flow Using the Lattice Boltzmann Method. International Journal for Numerical Methods in Fluids, 59, 753–765.
2. Benzi, R., Succi, S., Vergassola, M. 1992. The Lattice Boltzmann Equation: Theory and Applications. Physics Reports, 222(3), 145–197.
3. Chen, Shiyi., Doolen, Gary D 1998. Lattice Boltzmann Method for Fluid Flows. Annual review of fluid mechanics, 30(1), 329–364.
4. Chen Y., Xiangyangand W., Hanhua Z. 2021. A General Single-Node Second-Order Boundary Condition for the Lattice Boltzmann Method. Physics of Fluids, 33(4).
5. Fennema R.J. Chaudhry M.H. 1990. Explicit Methods for 2-D Transient Free Surface Flows. Journal of Hydraulic Engineering, 116(8), 1013–1034.
6. Hashemi A., Fischer, Fisher P., Francis L. 2018. Direct Numerical Simulation of Transitional Flow in a Finite Length Curved Pipe. Journal of Turbulence, 19(8), 664–682.
7. He, S., Seddighi, M. 2013. Turbulence in Transient Channel Flow. Journal of Fluid Mechanics, 715, 60–102.
8. Cheylan I., Favier J., Sagaut P. 2021. Immersed Boundary Conditions for Moving Objects in Turbulent Flows with the Lattice-Boltzmann Method.Pdf.
9. Khair A., Wang B.C., Kuhn David S. 2015. Study of Laminar–Turbulent Flow Transition under Pulsatile Conditions in a Constricted Channel. International Journal of Computational Fluid Dynamics, 29(9–10), 447–463.
10. Li Y., Huang P. 2008. A Coupled Lattice Boltzmann Model for Advection and Anisotropic Dispersion Problem in Shallow Water. Advances in Water Resources, 31(12), 1719–1730.
11. Liang S.J., Tang, J.H., Wu M.S. 2008. Solution of Shallow-Water Equations Using Least-Squares Finite-Element Method. Acta Mechanica Sinica/Lixue Xuebao, 24(5), 523–532.
12. Liu F.L.L.P., Fang, L. 2018. Non-Equilibrium Turbulent Phenomena in Transitional Channel Flows. Journal of Turbulence, 19(9), 731–753.
13. Liu H., Zhou G.J., Burrows R. 2009. Lattice Boltzmann Model for Shallow Water Flows in Curved and Meandering Channels. International Journal of Computational Fluid Dynamics, 23(3), 209–220.
14. Haifei L., Zhou J.G., Burrows R. 2009. Multi-Block Lattice Boltzmann Simulations of Subcritical Flow in Open Channel Junctions. Computers and Fluids, 38(6), 1108–1117.
15. Haifei L., Zhou J.G., Burrows R. 2010. Lattice Boltzmann Simulations of the Transient Shallow Water Flows. Advances in Water Resources, 33(4), 387–396.
16. Haifei L., Zhou J.G., Li M., Yanwei Z. 2013. Multi-Block Lattice Boltzmann Simulations of Solute Transport in Shallow Water Flows. Advances in Water Resources, 58, 24–40.
17. Marusic I., Joseph, D.D., Krishnan M. 2007. Laminar and Turbulent Comparisons for Channel Flow and Flow Control. Journal of Fluid Mechanics, 570, 467–477.
18. Mojab S., Pollard M., Pharoah A., Beale J.G., S.B.,

Hanff, E.S. 2014. Unsteady Laminar to Turbulent Flow in a Spacer-Filled Channel. Flow, Turbulence and Combustion, 92(1–2), 563–577.

19. Wang N., Ni W., Liu H. 2024. Geometrical Wetting Boundary Condition for Complex Geometries in Lattice Boltzmann Color-Gradient Model.
20. Noble, D., Chen R., Georgiadis S.J.G., Buckius, R.O. 1995. A Consistent Hydrodynamic Boundary Condition for the Lattice Boltzmann Method. Physics of Fluids, 7(1), 203–209.
21. Pargal, S., Yuan J., Brereton, G. 2021. Impulse Response of Turbulent Flow in Smooth and Riblet-Walled Channels to a Sudden Velocity Increase. Journal of Turbulence, 22(6), 353–379.
22. Peng Y., Zhou J.G., Burrows R. 2011. Modelling Solute Transport in Shallow Water with the Lattice Boltzmann Method. Computers and Fluids, 50(1), 181–188.
23. Qian Y.H., D'Humières D., Lallemand P. 1992. Lattice Bgk Models for Navier-Stokes Equation. Epl, 17(6), 479–484.
24. De Rosis A. 2023. A Comparison of Lattice Boltzmann Schemes for Sub-Critical Shallow Water Flows. Physics of Fluids, 35(4).
25. Schlatter P., Stolz S., Kleiser L. 2006. Large-Eddy Simulation of Spatial Transition in Plane Channel Flow. Journal of Turbulence, 7(September 2014), 1–24.
26. Tubbs K.R., Frank T.C., Tsai. 2009. Multilayer Shallow Water Flow Using Lattice Boltzmann Method with High Performance Computing. Advances in Water Resources, 32(12), 1767–1776.
27. Venturi S., Di Francesco S., Geier M., Manciola P. 2020. A New Collision Operator for Lattice Boltzmann Shallow Water Model: A Convergence and Stability Study. Advances in Water Resources, 135, 103474.
28. Xia Z., Shi Y., Zhao Y. 2015. Assessment of the Shear-Improved Smagorinsky Model in Laminar-Turbulent Transitional Channel Flow. Journal of Turbulence, 16(10), 925–936.
29. Yoon T.H., Kang S.-K. 2004. Finite Volume Model for Two-Dimensional Shallow Water Flows on Unstructured Grids. Journal of Hydraulic Engineering, 130(7), 678–688.
30. Zhou J.G. 2002. A Lattice Boltzmann Model for the Shallow Water Equations. Chaos, 191, 3527–3539.
31. Zhou J.G. 2002. A Lattice Boltzmann Model for the Shallow Water Equations with Turbulence Modeling. International Journal of Modern Physics C, 13(8), 1135–1150.
32. Zhou J.G. 2004. Lattice Boltzmann Methods for Shallow Water Flows. Springer.
33. Zou Q., He X. 1997. On Pressure and Velocity Boundary Conditions for the Lattice Boltzmann BGK Model. Physics of Fluids, 9(6), 1591–1598.